



PHILCO

A SUBSIDIARY OF *Ford Motor Company*

AERONUTRONIC DIVISION

FACILITY FORM 602

N66-23807

(ACCESSION NUMBER) _____

99 (PAGES)

CR-71769 (NASA OR OR TMX OR AD NUMBER)

(THRU) _____

(CODE) _____

06 (CATEGORY)

GPO PRICE \$ _____

CFSTI PRICE(S) \$ _____

Hard copy (HC) 3.00

Microfiche (MF) .75

Under Contracts: NOnr 3560(00)
ARPA Order No. 273/11-7-64 and
Subcontract No. 951260
NAS7-100
Task Order No. RD-38

31 August 1965

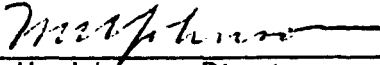
**This work was performed for the Jet Propulsion Laboratory,
California Institute of Technology, sponsored by the
National Aeronautics and Space Administration under
Contract NAS7-100.**

SCIENTIFIC REPORT

ABSORPTION BY CO₂ BETWEEN 5400 AND 6600 cm⁻¹
(1.6 Micron Region)

Prepared for: Advanced Research Projects Agency
Washington 25, D.C.

Prepared by: Darrell E. Burch
David A. Gryvnak
Richard R. Patty

Approved: 
M. H. Johnson, Director
Physics Laboratory

"This material is the result of tax-supported research and as such
may be freely reprinted with the customary crediting of the source."

ABSTRACT

23807

The absorption by 28 different samples of CO_2 and $\text{CO}_2 + \text{N}_2$ in the $5400\text{-}6600\text{ cm}^{-1}$ ($1.6\ \mu$) region has been studied by the use of a spectrometer having a spectral resolution between approximately 0.5 and 1.3 cm^{-1} . Samples were contained in two different absorption cells; one having a maximum path of 933 meters and used at a maximum pressure of 2.5 atm. The other was used at paths as long as 32.9 meters and at pressures as high as 14.6 atm. Photographs of the spectra of all the samples as well as a table of transmittance versus wavenumber are included. Also presented is a table of integrated absorptance $\int_{\nu'}^{\nu} A(\nu) d\nu$ versus ν , where approximately 380

values are tabulated for the largest samples.

Author

ACKNOWLEDGMENT

The research described in this report is a result of joint support under Contract NOnr 3560(00), ARPA Order No. 273/11-7-64 and Subcontract No. 951260, under NASA Contract NAS7-100, Task Order No. RD-38.

The authors would like to acknowledge the assistance of Mr. Francis Gates who performed much of the work in getting the instruments assembled and in reducing the data. Dr. William S. Benedict of Johns Hopkins University made many worthwhile suggestions and is responsible for the identification of new absorption bands. Several helpful discussions with Drs. Louise Gray and Lewis Kaplan of Jet Propulsion Laboratory are also greatly appreciated.

TABLE OF CONTENTS

<u>Section</u>		<u>Page</u>
1	INTRODUCTION AND SUMMARY	1-1
2	EXPERIMENTAL METHODS	2-1
	2.1 GAS SAMPLING	2-1
	2.2 RECORDING AND CALIBRATION OF SPECTRA	2-3
3	DISCUSSION OF ABSORPTION BANDS	3-1
	3.1 IDENTIFICATION AND FEATURES OF THE ABSORPTION BANDS	3-1
	3.2 BAND STRENGTHS	3-17
4	TABLE OF TRANSMITTANCES	4-1
5	TABLE OF INTEGRATED ABSORPTANCE	5-1
6	REFERENCES	6-1

LIST OF FIGURES

<u>Fig. No.</u>		<u>Page</u>
3-1	SPECTRUM OF THE $00^{\circ}3 \leftarrow 02^{\circ}0$ AND $00^{\circ}3 \leftarrow 10^{\circ}0$ BANDS FOR SAMPLE 1 IN THE REGION BETWEEN 5450 AND 5710 cm^{-1}	3-4
3-2	SPECTRUM OF THE 5800-6600 cm^{-1} REGION	3-5
3-3 to 3-6	SPECTRA OF THE 5900-6275 cm^{-1} REGION	3-6 to 3-9
3-7 to 3-10	SPECTRA OF THE 6275-6600 cm^{-1} REGION	3-10 to 3-13

LIST OF TABLES

<u>Table No.</u>	<u>Title</u>	<u>Page</u>
2-1	RESOLUTION SCHEDULES	2-4
3-1	CO ₂ BANDS BETWEEN 5500 AND 6600 cm ⁻¹	3-2
3-2	SAMPLE PARAMETERS ,	3-14 to 3-15
3-3	CALIBRATION LINES BETWEEN 5800 AND 6600 cm ⁻¹	3-16
3-4	BAND STRENGTHS	3-19
4-1	TABLE OF TRANSMITTANCES	4-3 to 4-50
5-1	TABLE OF INTEGRATED ABSORPTANCE	5-2 to 5-9

SECTION 1

INTRODUCTION AND SUMMARY

Most of the absorption by CO_2 in the $5400\text{-}6600\text{ cm}^{-1}$ region is due to four summation bands ($06^\circ 1$, $14^\circ 1$, $22^\circ 1$, and $30^\circ 1$) and their associated difference bands. Besides these bands, there are a few others which are extremely weak and are not observable except for very large samples. But, although they are very weak, they may produce most of the absorption over a few small intervals.

At present there is particular interest in these CO_2 bands because a detailed knowledge of them is important in the investigation of the atmospheres of Mars and Venus. This wavenumber region is useful since it is relatively free of absorption by other gases which occur in the earth's atmosphere; therefore, spectra of the planets can be obtained from ground level. Furthermore, the CO_2 bands are sufficiently weak that the absorption of the radiation as it passes through the earth's atmosphere is small and can be accounted for.

Howard, Burch and Williams¹ have made some quantitative measurements on the absorption in this region, but the use of their data is limited by the relatively low spectral resolution. Courtoy² has measured the positions of several hundred absorption lines with very good accuracy and has identified many bands which had not been observed previously; but only limited information about the amount of absorption by a given sample can be obtained from these results. Kuiper³ has also investigated the absorption by large samples; but his measurements were made with only moderate resolution and with samples at pressures of several atmospheres.

Because of the limitations of the previous work, there was still need for data on samples covering wide ranges of pressure and absorber thickness and with resolution sufficiently good that at least some lines from most of the bands could be resolved. The present investigation was undertaken for the purpose of obtaining these data. A long absorption cell with possible paths as great as 933 meters enabled us to study samples having very large absorber thickness at pressures which are not so great as to smooth out the structure in the band. Because of the long paths, we were able to observe and identify five new CO₂ bands in this region which have not been reported previously.

A shorter cell was also used to investigate samples at higher pressures in order that band strengths could be measured easily. The strengths of the more important bands were determined and the results are tabulated in Section 3. The widths of many of the lines can also be determined from "curves of growth" of the average absorptance over relatively narrow intervals. Once the strengths and widths of the lines have been found, the absorptance at any wavenumber can be calculated for a great variety of samples, even though they may be non-uniform in temperature and pressure.

Spectra of 28 samples with pressures ranging from 0.02 to 14.6 atmospheres and with path lengths from 4 to 933 meters have been reproduced and digitized. The reproduced spectra are shown in Section 3, and a table of transmittance $T(\nu)$ versus wavenumber ν is presented in Section 4. Section 5 contains a table of $\int_{\nu'}^{\nu} A(\nu) d\nu$, the integrated absorptance, versus ν . ν' is on the low wavenumber side of the region considered for a given sample, and the tabulations are made for approximately 380 different values of ν for the largest samples.

SECTION 2

EXPERIMENTAL METHODS

2.1 GAS SAMPLING

Samples of CO_2 and $\text{CO}_2 + \text{N}_2$ were contained in two different absorption cells which have been described previously.⁴ The longer cell has a base length of approximately 30 meters and was used at as many as 32 passes, giving a total path length of 933 meters. It is approximately 0.9 meters in diameter and can be evacuated to less than 1 micron of Hg or pressurized to as much as 2.5 atmospheres. The shorter cell has a base length of approximately 1 meter and was used at as many as 32 passes. It can be evacuated or pressurized to as much as 15 atmospheres.

The CO_2 was drawn from the vapor in a dewar which contained both liquid and vapor maintained at a temperature less than about -20°C by a relief valve which kept the pressure from exceeding 300 psig. We found that there was considerably less H_2O in samples drawn from the vapor over the liquid rather than from the liquid. The H_2O content was also much lower than in samples obtained from commercial cylinders at room temperature. The amount of H_2O in the N_2 was much less than that in the CO_2 , and it was not necessary to take extreme care to reduce the amount of H_2O put into the sample with the N_2 . It was drawn off as a liquid into a heat exchanger where it evaporated and entered the cell.

$\text{CO}_2 + \text{N}_2$ mixtures were mixed in the cell. CO_2 was introduced to the desired pressure; N_2 was then added and mixed by fans inside the absorption cells. No attempt was made to change the relative abundances of the different isotopes of C or O in the samples studied. It is probably safe to assume that the natural abundances of these isotopes were present (C^{12} , 98.9%; C^{13} , 1.1%; O^{16} , 99.76%; O^{17} , 0.04%; O^{18} , 0.20%). Some results discussed in a previous report⁵ indicate that the abundance of C^{13} was, in fact, about 1.1%. No check was made on the isotopes of O.

Sample pressures less than approximately 0.06 atm were measured with a U-tube oil manometer, and those in the range $0.06 < P < 2$ atm with a U-tube Hg manometer. All pressures > 2 atm were measured with a bourbon-type gauge. For all except the lowest pressures used, the errors arising from the uncertainty in the pressure measurements are probably negligible.

Since CO_2 varies significantly from a perfect gas at some of the higher pressures used in this investigation, it was necessary to account for the Van der Waals' forces giving rise to the deviation from a perfect gas. In calculating the absorber thickness u , the following equation was used:

$$u = W p L \frac{273}{296} \text{ (atm cm)}_{\text{STP}} \quad (2-1)$$

L is the geometrical path length in centimeters,
 p is the partial pressure of CO_2 in atmospheres,
 $273/296$ accounts for the difference in density between standard temperature and room temperature at which the measurements were made.

W is a correction term which accounts for the Van der Waals' forces in CO_2 and is given adequately for the pressures used in this investigation by

$$W = 1.00 + 0.0047 p. \quad (2-2)$$

In order to relate the pressure of a sample to the half-width of the absorption lines, it is necessary to account for the different broadening abilities of CO_2 and N_2 when dealing with mixtures of these two gases. Burch, Gryvnak and Williams⁶ have used an equivalent pressure P_e given by

$$P_e = 1.3 p + (P - p), \quad (2-3)$$

where P is the total pressure. It is noted that the equivalent pressure approaches the total pressure for a very dilute mixture of CO_2 in N_2 , which is a good approximation to the earth's atmosphere.

Since the simple classical theory predicts that the half-width of a line is proportional to the density of molecules, Equation (2-3) should probably be modified to account for the non-linearity between the density of CO_2 and its partial pressure. No correction is necessary for N_2 since it behaves much more like a perfect gas. The adjustment was made in the following way:

$$P_e = 1.3 W p + (P-p). \quad (2-3')$$

The self-broadening factor 1.3 is not valid in all portions of the spectrum. But in a detailed study of the shapes of collision-broadened lines which will be described in a separate report,⁷ we found that it is satisfactory in regions where most of the absorption is due to lines whose centers are a few tenths of a cm^{-1} away. Therefore, it probably can be used throughout most of the region covered by this report. However, it should be considerably greater in a region such as that between 7100 cm^{-1} and the head of the 00^0_3 band at approximately 6990 cm^{-1} where the absorption is due to the wings of lines whose centers are several cm^{-1} away.⁵ The difference in the self-broadening factor arises from the fact that the shape of the extreme wings of a self-broadened line is quite different from that of a nitrogen-broadened line.

2.2 RECORDING AND CALIBRATION OF SPECTRA

The spectra were obtained with an Ebert-type spectrometer whose main mirror has a 75 cm focal length. It utilized a small grating having a ruled area 64×64 mm with 600 lines/mm and blazed at 1.6 microns. The grating was used in the first order and a Si filter eliminated overlapping orders of shorter wavelength. A PbS cell cooled with liquid nitrogen was used as the detector. It was not necessary to cool the detector below dry ice temperature for operation in this wavelength region, but the dewar was designed to hold the liquid nitrogen for use at longer wavelengths. Cooling by liquid nitrogen was, therefore, more convenient and was used since the signal-to-noise ratio was approximately the same at both temperatures.

The spectrometer is "home made" and was contained in a tank which could be evacuated to essentially eliminate absorption due to atmospheric gases outside of the absorption cell. The spectrometer tank, as well as another tank containing the radiation source and chopper, were connected to the absorption cell by means of flexible bellows so that all of the optical path external to the absorption cell could be evacuated.

Three different resolution schedules were used in recording the spectra: the approximate spectral slitwidths for each schedule at three different wavenumbers are given in Table 2-1.

TABLE 2-1
RESOLUTION SCHEDULES

ν (cm^{-1})	Spectral Slitwidth (cm^{-1})		
	Schedule A	Schedule B	Schedule C
5900	0.49	0.78	1.07
6200	0.55	0.88	1.22
6500	0.61	0.97	1.35

Resolution Schedule A was used in a few regions of the spectrum to resolve closely spaced lines; but because of the small signal available while using this schedule, considerable time was required to scan even a short spectrum. Therefore, B, which represents a compromise between resolution and scanning time, was used for the majority of the data. Schedule C was used for some spectra of samples at several (32) passes of the absorption cell for which the signal was low. The schedule used for each spectrum is listed in Table 3-2.

CO_2 and CH_4 lines whose positions are well known, or could be calculated, were used for the wavenumber calibration of the spectra. The calibration lines are separated by an average of about 10 cm^{-1} , which is sufficiently close that the spectrum could be assumed to be linear between them. All the lines used for calibration between 5800 and 6600 cm^{-1} are listed in Table 3-3, and their positions are shown on the spectra in Section 3. The calibration lines used between 5500 and 5700 cm^{-1} are shown in Fig. 3-1.

Background curves were obtained with the absorption cell evacuated for each number of passes for which sample spectra were obtained. The background curves were different for different numbers of passes since the reflectivity of the mirrors in the multiple-pass optics varies with wavenumber. The appropriate background curve, which represents 100 percent transmittance, was then fitted to each spectrum and traced on it. All the sample spectra extended beyond the region of absorption on both ends of the band so that dependable "tie-points" between a spectrum and its background could be established. The transmittance was determined from the ratio of the deflection of the sample spectrum to that of the background curve at the same wavenumber.

Each spectrum was examined and compared with others as a check for consistency. Small changes were made to account for H_2O absorption. The corrections could be made reasonably accurately by comparing the

spectra with those of $\text{H}_2\text{O} + \text{N}_2$ samples at the proper path lengths and pressures. The corrected spectra were then replotted and are shown in Section 3. As each spectrum was being replotted, pairs of values related to transmittance and wavenumber were punched on IBM cards which served as input for a computer program used to calculate transmittance and integrated absorptance as a function of wavenumber.

SECTION 3

DISCUSSION OF ABSORPTION BANDS

3.1 IDENTIFICATION AND FEATURES OF THE ABSORPTION BANDS

All of the CO₂ bands which one might expect to produce appreciable absorption in the region from 5400 to 6600 cm⁻¹ are listed in Table 3-1. The positions of the band centers of most of the bands are taken from Courtoy,² while centers of the others were calculated from energy levels tabulated by Stull, Wyatt and Plass.⁸ In the notation for the transitions the lower level is omitted when it is 00⁰0. There are probably other very weak bands in this region, particularly some from transitions from higher energy levels, which could be observed with better resolution and long paths. However, their contribution is certainly small at room temperature or below. The bands listed are limited to those observed by Courtoy² plus those we observed and were able to identify with reasonable certainty.

With the exception of five of the weaker bands listed, all those in this region arise from transitions in which there is a change of one in ν_3 , the quantum number associated with ν_3 ($\Delta\nu_3 = 1$). Since for CO₂, $\nu_1 \approx 2\nu_2$, all bands for which $2\Delta\nu_1 + \Delta\nu_2$ is constant occur close to each other if $\Delta\nu_3$ is the same. $2\Delta\nu_1 + \Delta\nu_2 = 6$ for all the bands listed in Table 3-1 having $\Delta\nu_3 = 1$. Since ν_1 is not exactly equal to $2\nu_2$, but slightly larger, the bands having the largest change in ν_1 occur at slightly higher frequencies. $\nu_1 = 1388.2$ and $\nu_2 = 667.4$ for C¹²O₂¹⁶.

TABLE 3-1

CO₂ BANDS BETWEEN 5500 and 6600 cm⁻¹

Band Center cm ⁻¹	Transition	Species
5584.28 ^a	00 ⁰ 3←10 ⁰ 0	12, 16, 16 ^b
5687.05 ^a	00 ⁰ 3←02 ⁰ 0	12, 16, 16
5857.59 ^a	02 ⁰ 2	12, 16, 18
5951.53	06 ⁰ 1	13, 16, 16
5959.57 ^a	10 ⁰ 2	12, 16, 18
6020.75	07 ¹ 1←01 ¹ 0	12, 16, 16
6075.93	06 ⁰ 1	12, 16, 16
6088.16	15 ¹ 1←01 ¹ 0	13, 16, 16
6119.56	14 ⁰ 1	13, 16, 16
6196.12	15 ¹ 1←01 ¹ 0	12, 16, 16
6227.88	14 ⁰ 1	12, 16, 16
6241.93	22 ⁰ 1	13, 16, 16
6243.54	23 ¹ 1←01 ¹ 0	13, 16, 16
6308.15	24 ⁰ 1←02 ⁰ 0	12, 16, 16
6347.81	22 ⁰ 1	12, 16, 16
6356.25	23 ¹ 1←01 ¹ 0	12, 16, 16
6363.58	30 ⁰ 1	13, 16, 16
6397.51	31 ¹ 1←01 ¹ 0	13, 16, 16
6503.05	30 ⁰ 1	12, 16, 16
6536.43	31 ¹ 1←01 ¹ 0	12, 16, 16
6538.03 ^a	03 ¹ 2	12, 16, 16

^aTo the knowledge of the authors, these bands have not been observed previously; band centers were calculated from energy levels tabulated by Stull, Wyatt and Plass.⁸ Centers for all other bands are taken from Courtoy.²

^bNumbers represent isotopes of C, O, and O, respectively.

Because of anharmonicity, a combination or fundamental band usually occurs at a slightly higher wavenumber than its associated difference band which arises from a transition from an excited state with the changes in all three quantum numbers the same. However, the displacement of the bands varies from one band to another, depending on Fermi resonance. It can be seen that the 30^0_1 and 22^0_1 bands occur at lower wavenumbers than their associated difference bands arising from transitions from the 01^1_0 state. However, as more frequently occurs, the opposite is true for the 14^0_1 and 06^0_1 bands.

The 02^0_2 and 10^0_2 bands of $C^{12}O^{16}O^{18}$ are forbidden for $C^{12}O_2^{16}$; but they appear because of the asymmetry of the $C^{12}O^{16}O^{18}$ molecule. The $00^0_3 \leftarrow 10^0_0$ and the $00^0_3 \leftarrow 02^0_0$ bands occur near each other since the upper level is common and $2\Delta v_1 + \Delta v_2$ is the same for both bands. A replotted spectrum of these bands¹ is shown in Figure 3-1; it was recorded for the largest sample studied.

A replotted spectrum of the region from approximately 5800 to 6600 cm^{-1} is shown in Figure 3-2 for the same sample. The positions of the centers of many of the bands are indicated. Spectra of the remainder of the samples are shown in Figures 3-3 through 3-6 and 3-7 through 3-10 for the spectral regions 5900 to 6275 cm^{-1} and 6275 to 6600 cm^{-1} , respectively. The numbers appearing in rectangles are the numbers assigned to the samples which are described in Table 3-2, the table of sample parameters.

The other numbers appearing in some of the spectra refer to the lines used in the wavenumber calibration. The positions of these lines are given in Table 3-3.

Portions of the spectra of some of the samples for which the absorption $A(\nu)$ was very small have been omitted. The spectra were "nested" in order to conserve space, and no attempt was made to put them in any particular order.

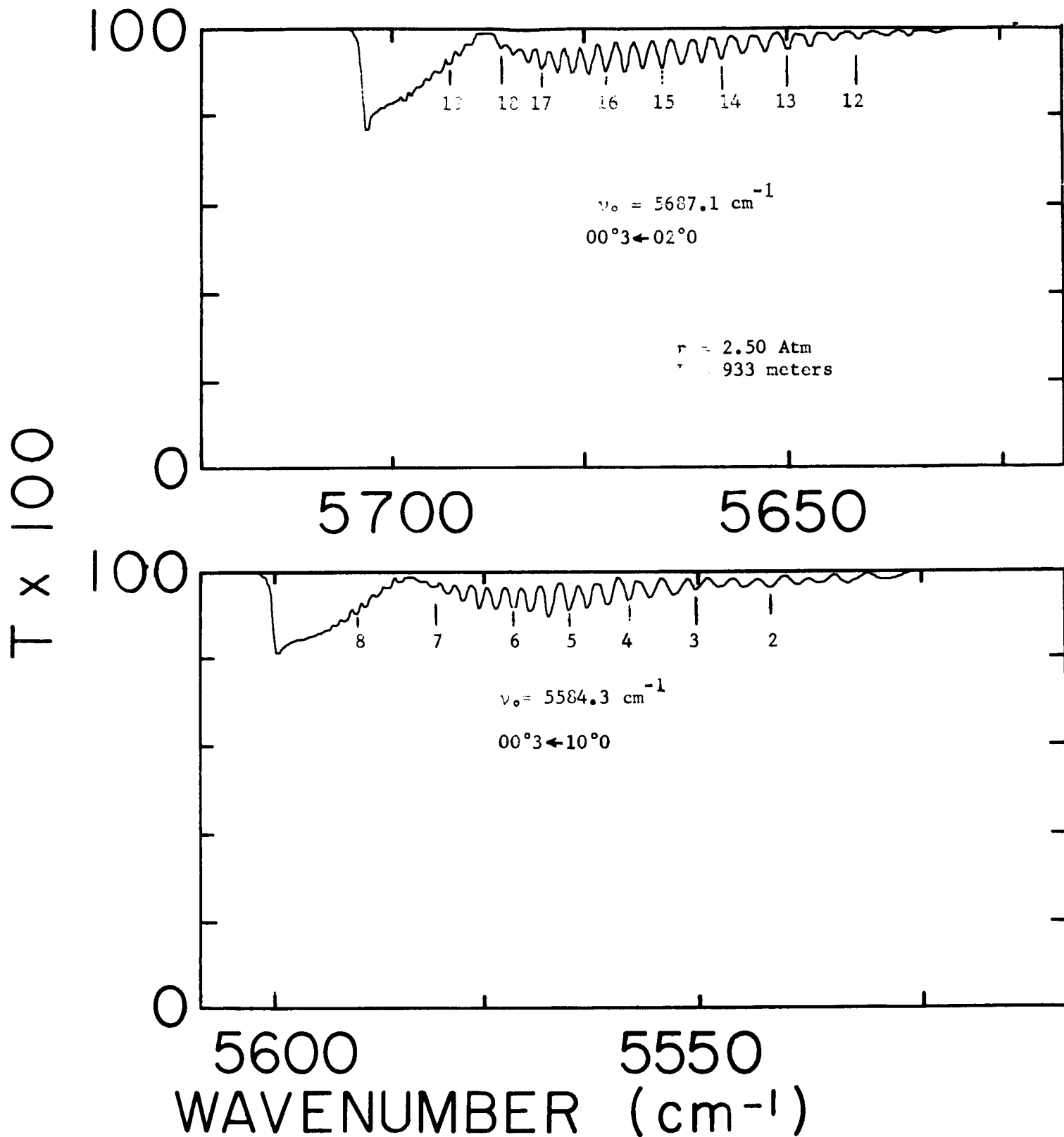


FIGURE 3-1 SPECTRUM OF THE $00^\circ 3 \leftarrow 02^\circ 0$ AND $00^\circ 3 \leftarrow 10^\circ 0$ BANDS FOR SAMPLE 1 IN THE REGION BETWEEN 5450 AND 5710 cm^{-1} .

The lines that are numbered were used in calibration and their wavenumber positions (cm^{-1}) are;

1 5507.8 (H_2O)	6 5571.7	11 5621.6 (H_2O)	16 5672.3
2 5541.8	7 5581.1	12 5641.1	17 5680.3
3 5550.2	8 5590.5	13 5649.8	18 5685.5
4 5558.1	9 5602.8 (H_2O)	14 5658.1	19 5692.0
5 5565.2	10 5614.0 (H_2O)	15 5665.5	

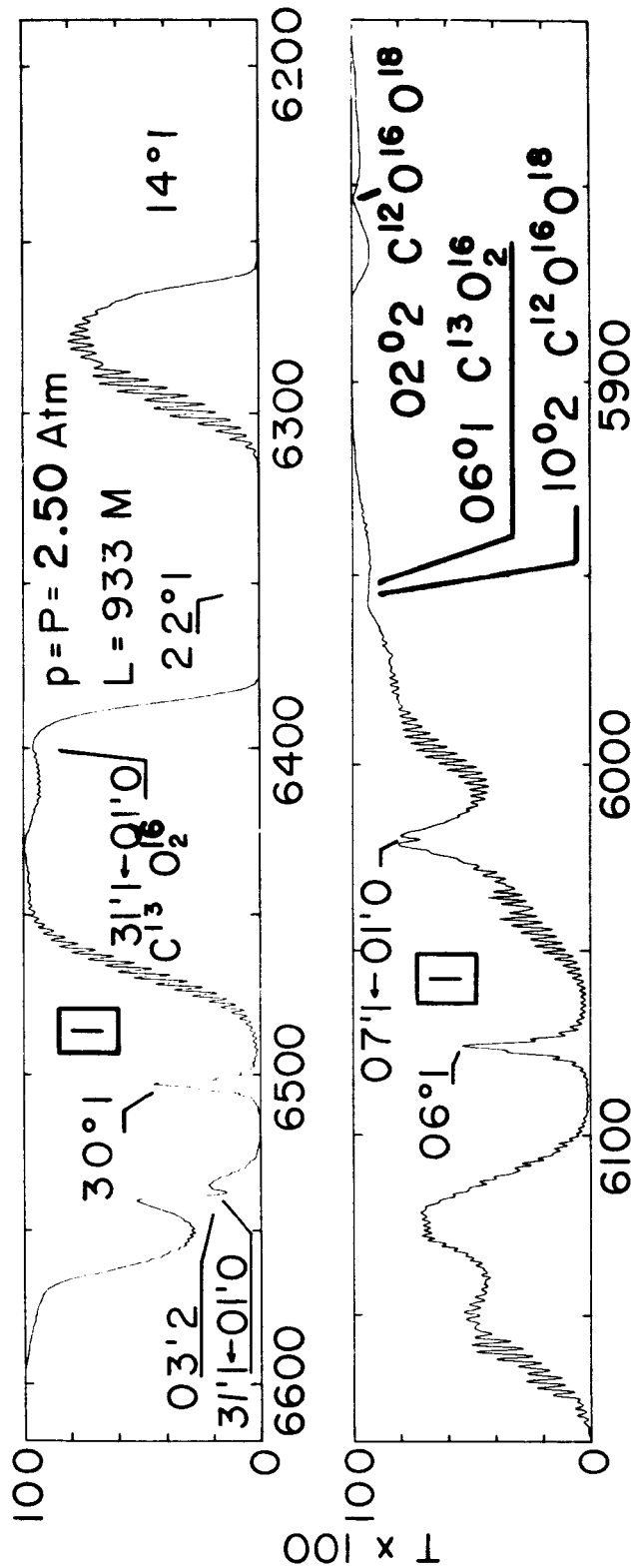


Fig. 3-2. WAVELENGTH (cm⁻¹)

FIGURE 3-2 SPECTRUM OF THE 5800 - 6600 cm⁻¹ REGION

The centers of several of the bands are indicated.
 The species is C₁₂O₁₆ when it is not indicated.

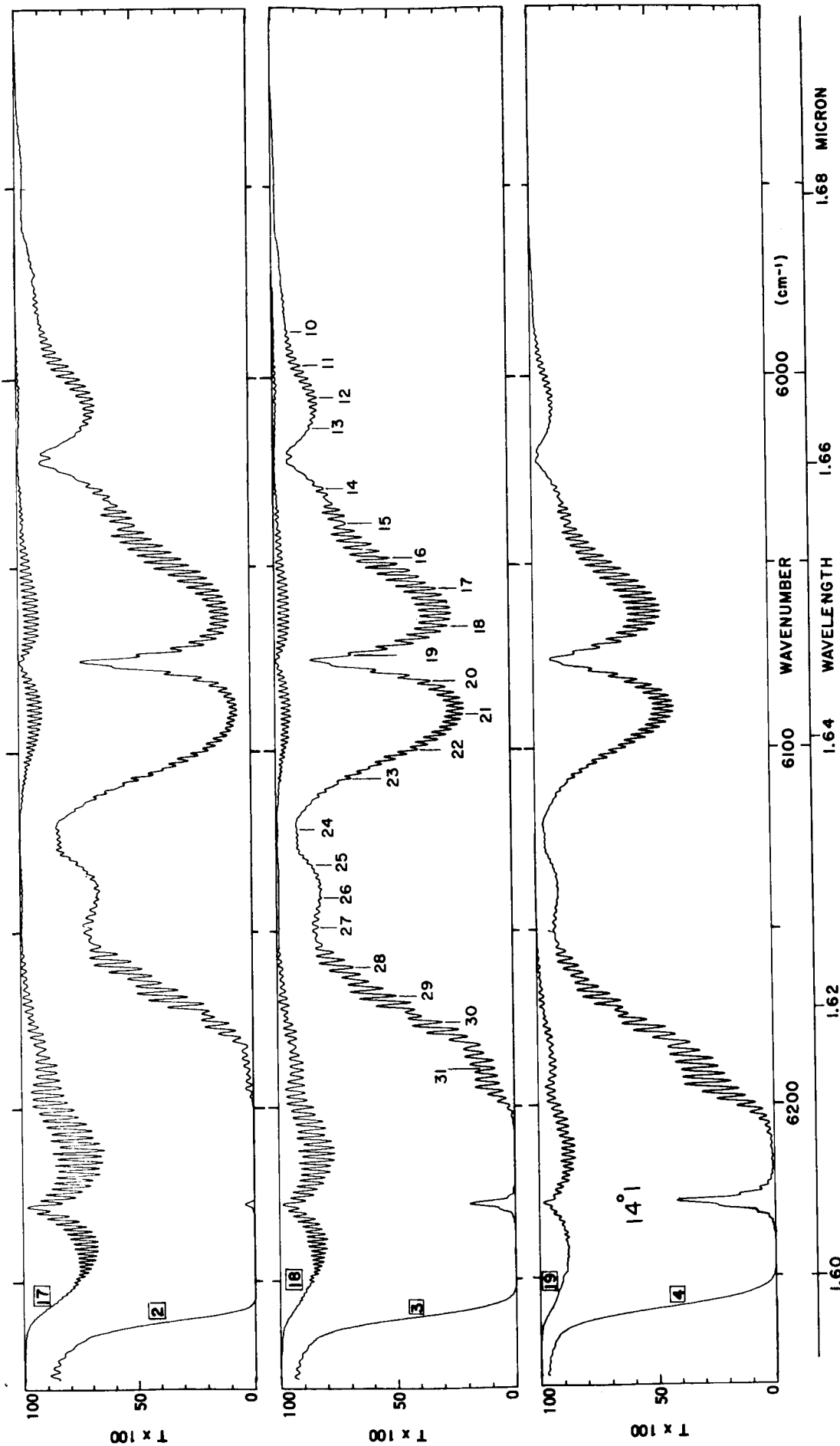


Fig. 3-3

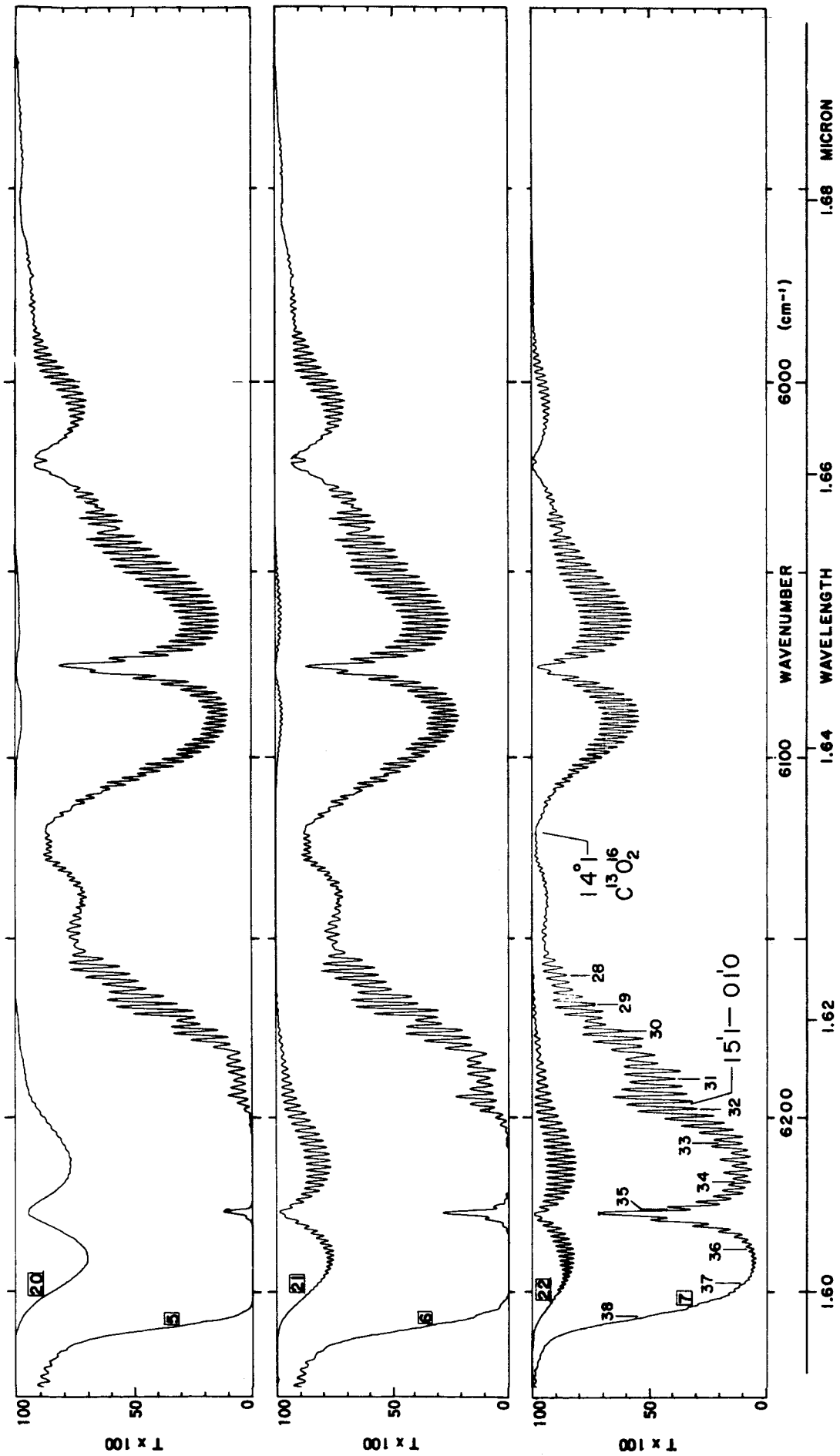


Fig. 3-4

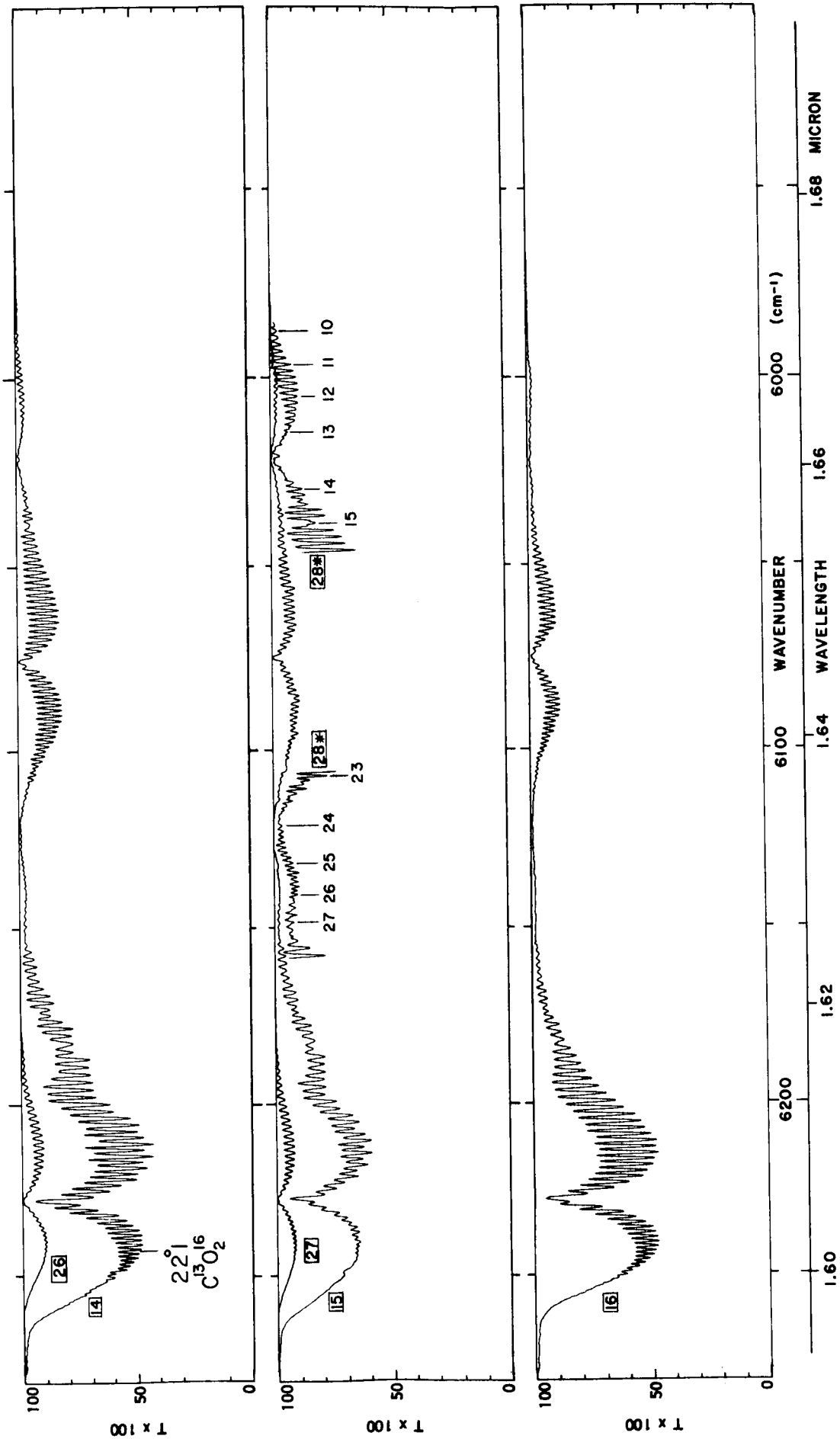


Fig. 3-5

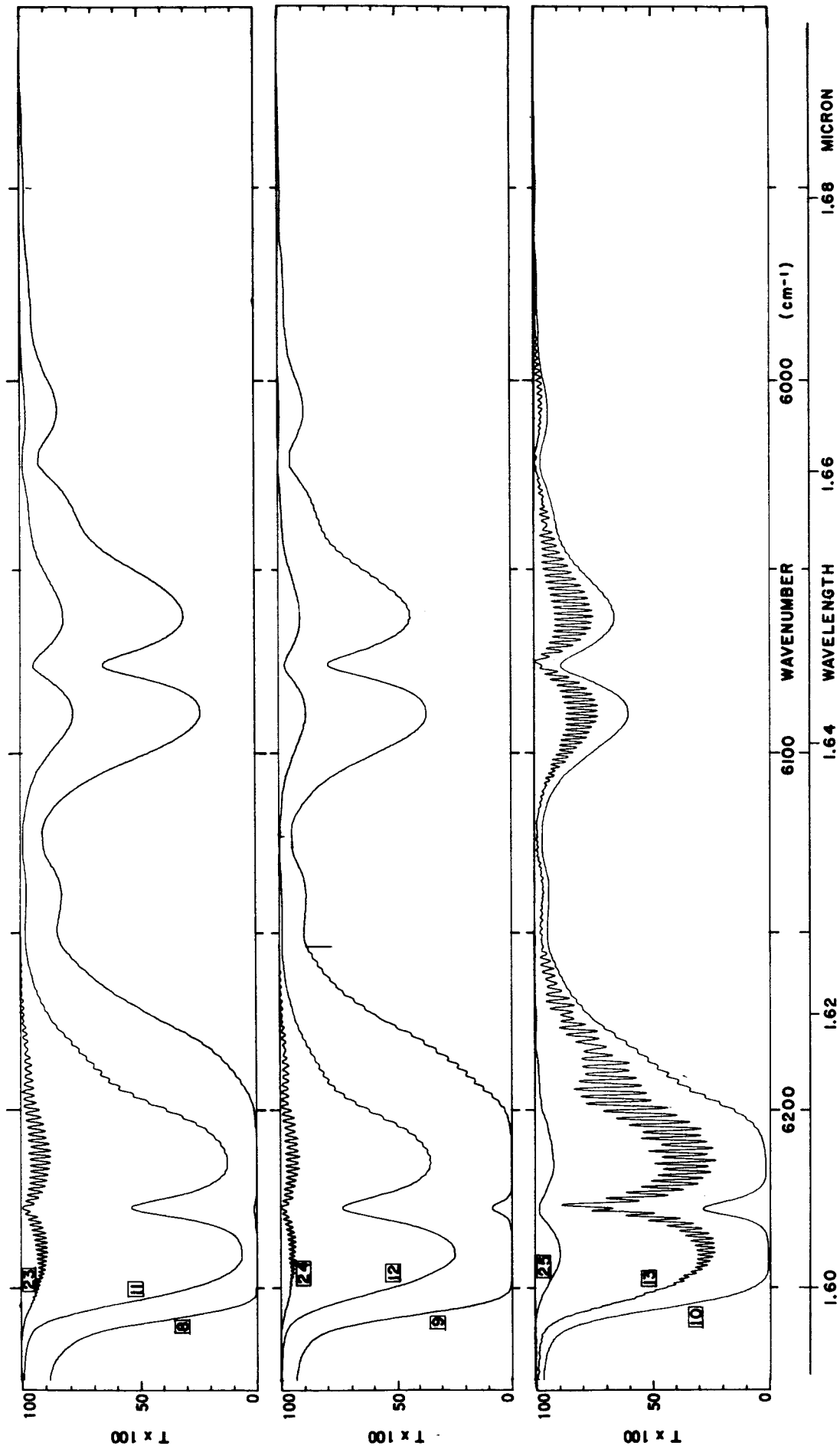


Fig. 3-6

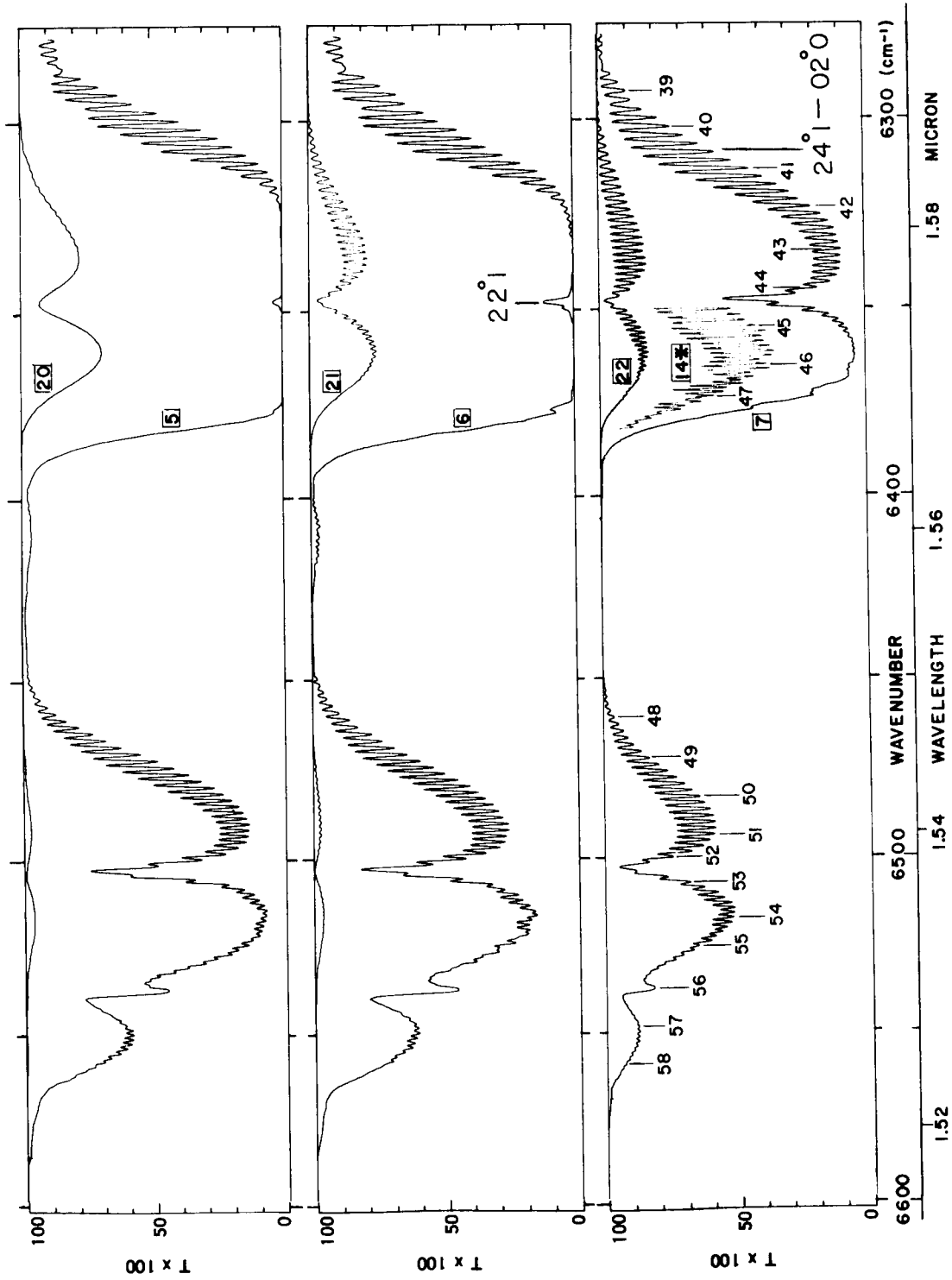


Fig. 3-7

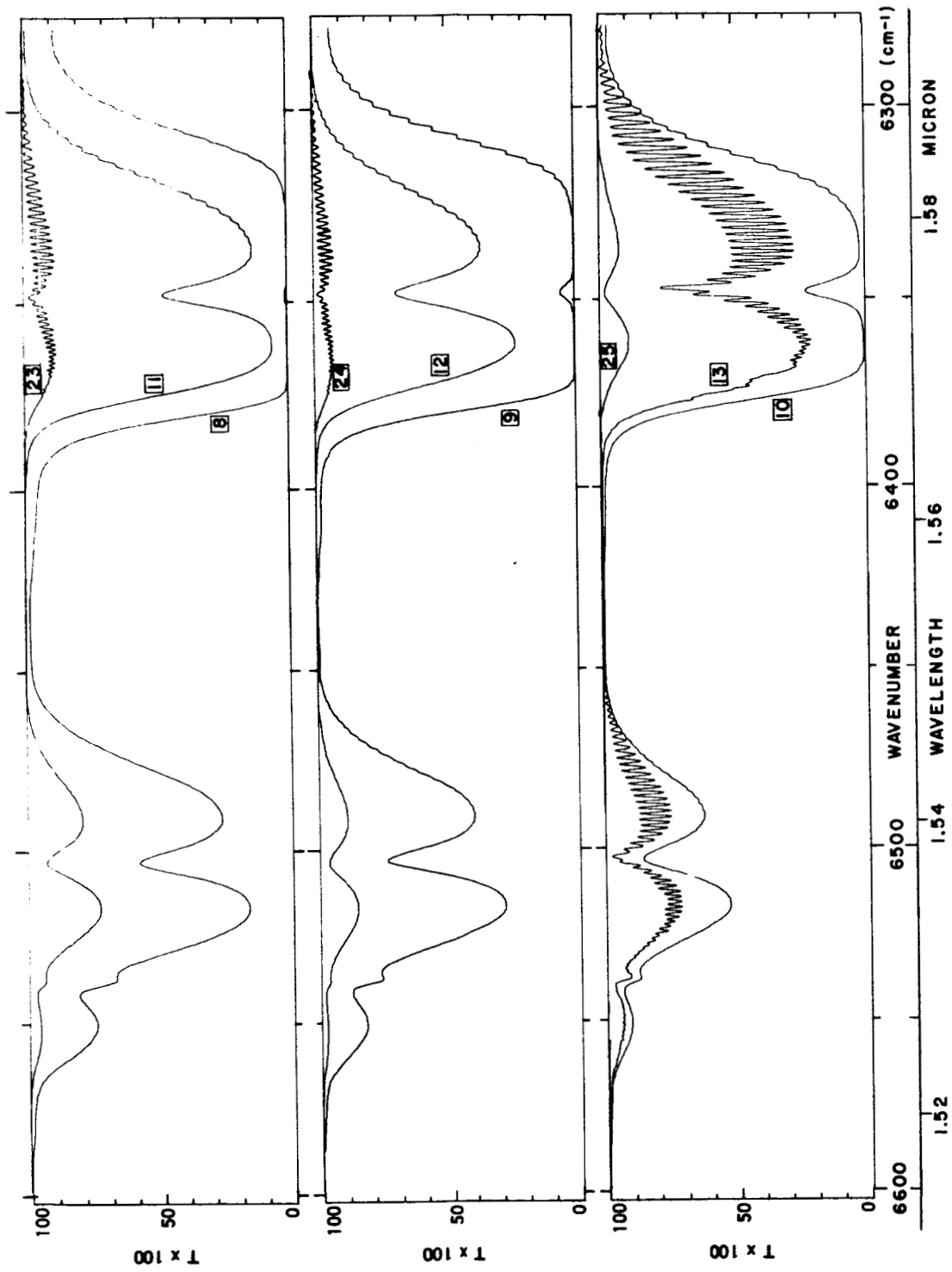


Fig. 3-8

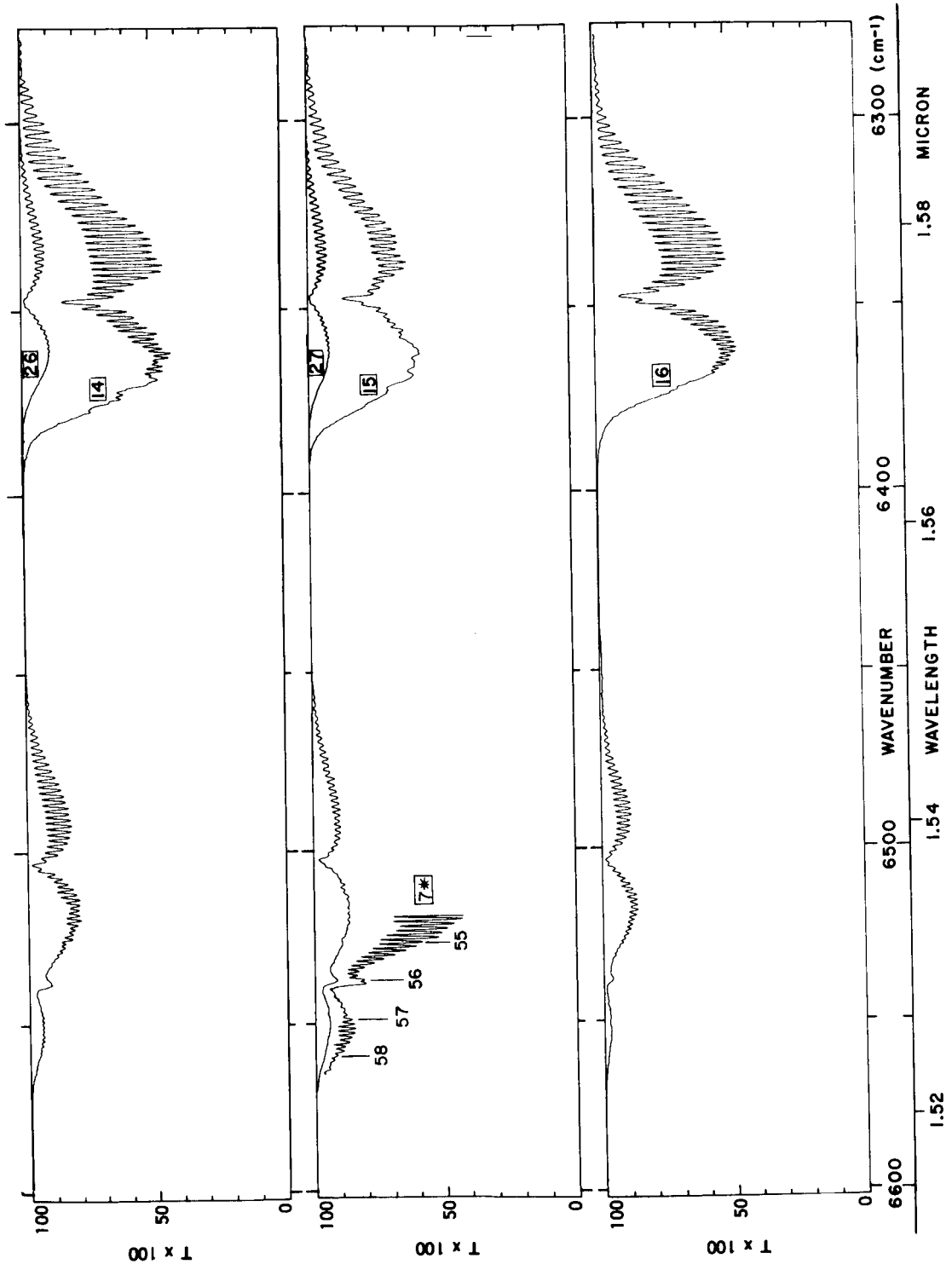


Fig. 3-9

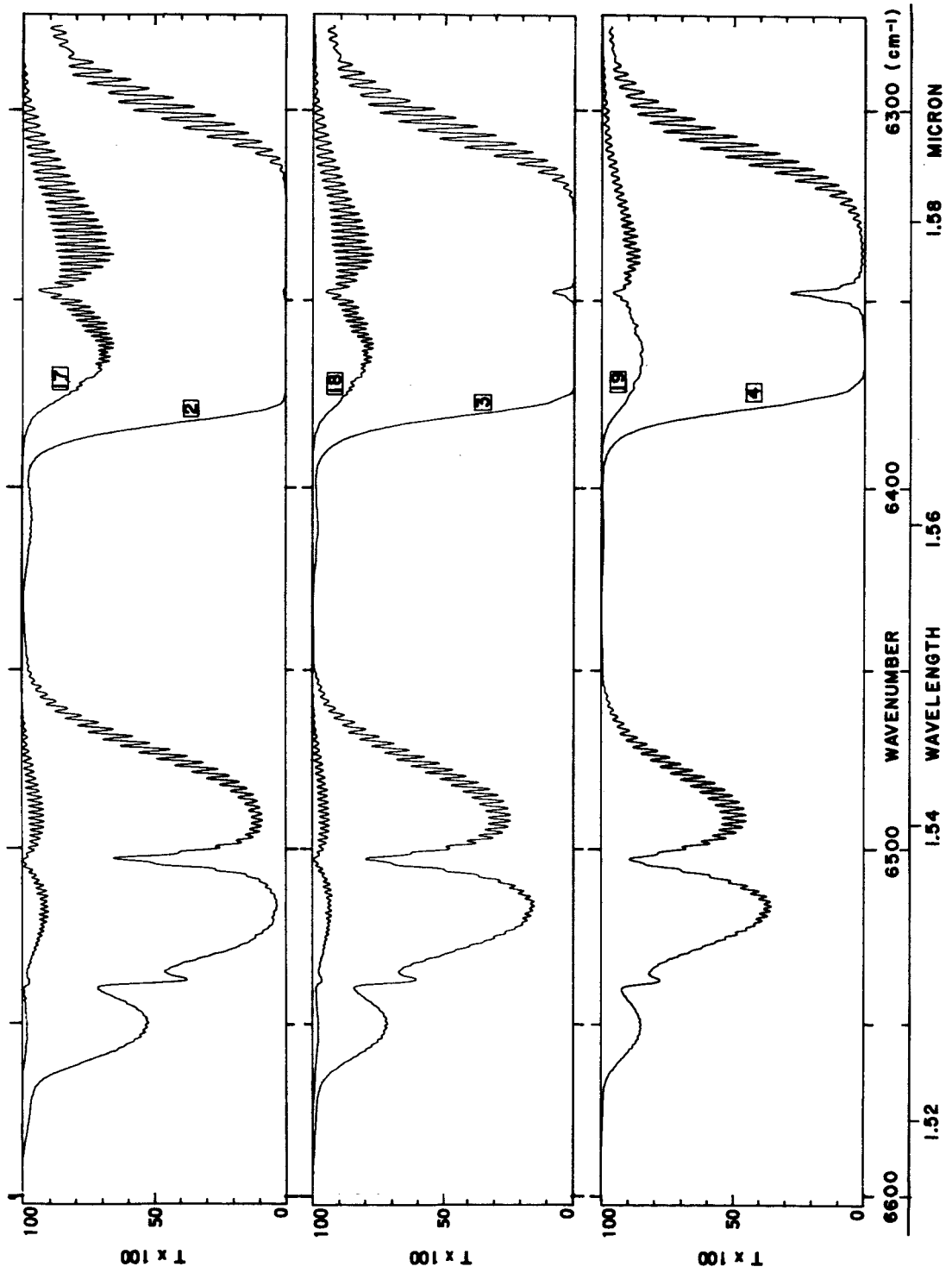


Fig. 3-10

Table 3-2

SAMPLE PARAMETERS

Sam. No.	P	P	P _e	p	P	P _e
	torr	torr	torr	atm	atm	atm
1	1,900	1,900	2,500	2.50	2.50	3.29
2	1,920	1,920	2,520	2.53	2.53	3.32
3	1,920	1,920	2,520	2.53	2.53	3.32
4	1,900	1,900	2,500	2.50	2.50	3.29
5	1,522	1,522	1,995	2.00	2.00	2.62
6	760	760	992	1.000	1.000	1.31
7	760	760	992	1.000	1.000	1.31
7*	760	760	992	1.000	1.000	1.31
8	11,100	11,100	15,500	14.6	14.6	20.3
9	7,600	7,600	10,300	10.00	10.00	13.6
10	7,600	7,600	10,300	10.00	10.00	13.6
11	7,600	7,600	10,300	10.00	10.00	13.6
12	7,600	7,600	10,300	10.00	10.00	13.6
13	175	707	759	0.230	0.930	0.999
14	175	175	228	0.230	0.230	0.300
14*	175	175	228	0.230	0.230	0.300
15	88	88	114	0.116	0.116	0.150
16	58.5	743	761	0.0770	0.977	1.001
17	58.5	212	230	0.0770	0.279	0.303
18	58.5	58.5	76.1	0.0770	0.0770	0.1001
19	29.4	29.4	38.2	0.0387	0.0387	0.0503
20	506	9,800	9,960	0.665	12.9	13.1
21	506	506	659	0.665	0.665	0.865
22	17.8	223	228	0.0234	0.293	0.300
23	17.8	72	77.3	0.0234	0.0946	0.102
24	17.8	17.8	23.1	0.0234	0.0234	0.0304
25	165	9,800	9,850	0.217	12.9	13.0
26	165	710	760	0.217	0.934	1.000
27	165	165	214	0.217	0.217	0.283
28*	1,083	1,083	1,410	1.43	1.43	1.86

*These spectra were obtained with higher resolution for calibration purposes. No calculations were made for the transmittance and integral tables.

Table 3-2 (Cont'd)

Sam. No.	L Path m	u atm cm STP	Res. Sch.	Pages on which spectra appear	
				6600-6275 -1 cm	6275-5900 -1 cm
1	933	217,000	B	3-5	3-5
2	469	110,000	B	3-13	3-6
3	237	55,700	B	3-13	3-6
4	121	28,000	B	3-13	3-6
5	469	87,100	B	3-10	3-7
6	933	86,200	B	3-10	3-7
7	237	21,900	B	3-10	3-7
7*	237	21,900	A	3-12	
8	32.9	47,300	B	3-11	3-9
9	32.9	31,600	B	3-11	3-9
10	16.5	15,900	B	3-11	3-9
11	8.26	7,930	B	3-11	3-9
12	4.16	3,990	B	3-11	3-9
13	469	9,940	B	3-11	3-9
14	469	9,940	B	3-12	3-8
14*	469	9,940	A	3-10	
15	933	9,940	C	3-12	3-8
16	469	3,320	B	3-12	3-8
17	469	3,320	B	3-13	3-6
18	469	3,320	B	3-13	3-6
19	933	3,320	C	3-13	3-6
20	16.5	1,010	B	3-10	3-7
21	16.5	1,010	B	3-10	3-7
22	469	1,010	B	3-10	3-7
23	469	1,010	B	3-11	3-9
24	469	1,010	B	3-11	3-9
25	16.5	330	B	3-11	3-9
26	16.5	330	B	3-12	3-8
27	16.5	330	B	3-12	3-8
28*	237	31,300	A		3-8

Table 3-3

CALIBRATION LINES BETWEEN 5800 AND 6600 cm^{-1} .

Line No.	ν cm^{-1}	Line No.	ν cm^{-1}	Line No.	ν cm^{-1}
1	5891.3 M	21	6090.2	41	6313.0
2	5903.3 M	22	6100.1	42	6323.1
3	5915.1 M	23	6107.9	43	6334.4
4	5926.5 M	24	6121.9	44	6344.6
5	5938.1 M	25	6132.0	45	6354.5
6	5949.5 M	26	6141.1	46	6364.9
7	5960.8 M	27	6149.1	47	6373.4
8	5972.1 M	28	6160.2	48	6460.9
9	5983.1 M	29	6168.3	49	6472.3
10	5987.5	30	6175.8	50	6483.1
11	5996.4	31	6189.0	51	6493.4
12	6004.7	32	6197.4	52	6499.9
13	6014.4	33	6207.2	53	6506.9
14	6029.5	34	6218.1	54	6517.0
15	6038.9	35	6226.3	55	6525.1
16	6047.8	36	6237.4	56	6537.0
17	6056.5	37	6247.4	57	6547.9
18	6066.4	38	6256.4	58	6558.6
19	6074.4	39	6293.0		
20	6081.3	40	6302.1		

^MThe calibration lines designated with an M are CH_4 lines whose wavenumbers are taken from Mohler.⁹ The remaining lines are CO_2 with wavenumbers taken from Courtoy.²

3.2 BAND STRENGTHS

The strength, or intensity, of an absorption band is given by

$$S_{\nu} = \int K(\nu) d\nu, \quad (3-1)$$

where the integration is performed over all ν for which there is appreciable absorption. $K(\nu)$, the absorption coefficient, is defined in terms of $T'(\nu)$, the true transmittance which would be observed with infinite resolving power, by

$$T'(\nu) = \exp \left[-u K(\nu) \right], \text{ or } -\ln T'(\nu) = u K(\nu). \quad (3-2)$$

Of course, if more than one band contributes to the absorption at a given wavenumber, $K(\nu)$ used in Equation (3-1) must include only the portion due to the band whose strength is being determined. The method used to estimate the contributions of each band in overlapping regions is described below.

The strengths of the bands included in this report are essentially independent of pressure over the range of pressures used. However, as the pressure is increased the lines are broadened until at 14.6 atm., the maximum pressure used, the half-widths are of the order of 1 to 1.5 cm^{-1} , which is less than the spectral slitwidth used in obtaining most of the spectra. Consequently, the observed transmittance $T(\nu)$ is very nearly the true transmittance $T'(\nu)$. By equating these two quantities and combining Equations (3-1) and (3-2), we obtain

$$S_{\nu} = -\frac{1}{u} \int \ln T(\nu) d\nu. \quad (3-3)$$

Equation (3-3) was used to determine the strengths of the stronger bands listed in Table 3-1 from spectra of samples at pressures greater than about 10 atmospheres. At these pressures, $T(\nu) \approx T'(\nu)$ and Equation (3-3) can be used, provided $T(\nu)$ is not too small, in which case the integral gets very large. Of course, the measurements cannot be made very accurately from spectra in which $A(\nu) \equiv 1 - T(\nu)$ is too small because of the large uncertainty arising from noise or misplacement of the background curve. For small $A(\nu)$, $-\ln T(\nu) \approx A(\nu)$. When possible, spectra were chosen so that $0.3 \leq T(\nu) \leq 0.9$ over most of the band. It was not possible to use samples with sufficiently large absorber thickness in the shorter absorption cell to produce more than a few percent absorbance by the very weak bands. Therefore, the strengths of these bands were necessarily determined from spectra of samples contained in the longer absorption cell, although its maximum pressure is 2.5 atmospheres.

At this pressure $T'(v)$ may be quite different from $T(v)$; but Equation (3-3) can still be used, provided $A(v)$ is small. A discussion of the limitations of Equation (3-3) when dealing with samples at relatively low pressures is given in Reference 5.

For $\Sigma \leftarrow \Sigma$ bands (quantum number $\ell = 0$) of CO_2 , the strength S_m of a given line within a band is related to the band strength S_v by

$$S_m = S_v |m| \exp \left[-\frac{B'' m(m-1)}{k\theta} \right] / Q_r \quad (3-4)$$

$m = J + 1$ for the R-branch and $-J$ for the P-branch. B'' is the rotational constant of the lower state, k is Boltzmann's constant, θ is the temperature, and Q_r is the rotational partition function. The Q-branch is missing in $\Sigma \leftarrow \Sigma$ bands, and contains only about one percent of the strength of $\Pi \leftarrow \Pi$ bands ($\ell = 1$ as in $15^1 1 \leftarrow 01^1 0$). Equation (3-4) also gives the strengths of lines in the P- and R-branches of $\Pi \leftarrow \Pi$ bands. Gray and Selvidge¹⁰ have tabulated values of partition functions and relative line strengths for different types of CO_2 bands at several temperatures.

According to quantum theory¹¹, the relative strength of a difference band $v_1, v_2^{+1}, v_3 \leftarrow 0, 1^1 0$ to its associated summation band v_1, v_2^0, v_3 is given by

$$\begin{aligned} \frac{S_v(v_1, v_2^{+1}, v_3 \leftarrow 01^1 0)}{S_v(v_1, v_2^0, v_3)} &= 2 \exp(-hc 667.4/k\theta) \\ &= 0.078 \text{ for } \theta = 296^\circ\text{K}. \end{aligned} \quad (3-5)$$

h is Planck's constant, c is the speed of light, and the factor 2 arises from the double degeneracy of the $01^1 0$ state. 667.4 cm^{-1} is the difference between energy levels $01^1 0$ and $00^0 0$.

Equation (3-5) also relates the strength of any difference band to its associated summation or fundamental band if the proper degeneracy factor is used and 667.4 is replaced by the difference between the energy level $00^0 0$ and the lower level for the difference band.

The strengths of several of the bands in this region are given in Table 3-4. From Equations (2-1) and (3-3), we see that the units of band strength are $\text{atm}^{-1} \text{ cm}^{-1}$, with the STP referring to the absorber thickness and not to the temperature at which the measurement was made. All measurements were at room temperature near 296°K .

TABLE 3-4

BAND STRENGTHS

Band Center cm ⁻¹	Transition	Species ^a	STRENGTH (atm ⁻¹ cm ⁻¹ STP cm ⁻¹)		
			P-Branch (Multiply all numbers below by 10 ⁻⁴)	R-Branch	Entire Band
5584.28	00 ⁰ 3-10 ⁰ 0	12,16,16	0.10 ± 0.02	0.09 ± 0.01	0.19 ± 0.03
5687.05	00 ⁰ 3-02 ⁰ 0	12,16,16	0.10 ± 0.02	0.10 ± 0.01	0.20 ± 0.03
5857.59	02 ⁰ 2	12,16,18	0.046 ± 0.006	0.056 ± 0.006	0.102 ± 0.011
6075.93	06 ⁰ 1	12,16,16	6.3 ± 0.5	7.0 ± 0.5	13.3 ± 1.0
6227.88	14 ⁰ 1	12,16,16	56 ± 6	63 ± 3	119 ± 9
6347.81	22 ⁰ 1	12,16,16	55 ± 4	63 ± 4	118 ± 8
6503.05	30 ⁰ 1	12,16,16	6.5 ± 0.4	7.0 ± 0.4 ^b	13.5 ± 0.8 ^b

^a Numbers denote isotopes of C, O, and O, respectively. The strengths are based on samples containing a mixture of all isotopic species, not just the one indicated.

^b Strengths of R-branch and of entire band were calculated from measured strength of P-branch by assuming 48% of strength is in P-branch.

The strengths of the $00^03 \leftarrow 10^00$ and $00^03 \leftarrow 02^00$ bands were determined from the spectrum shown in Figure 3-1. There were a few H_2O lines in the region of the $00^03 \leftarrow 10^00$ band in the original spectrum because of the trace of H_2O impurity in the sample. The spectrum was modified to account for the H_2O before it was replotted and digitized. Possible errors in accounting for the H_2O absorption increase the uncertainty in the measurement of the strengths by a few percent. Since the average absorptance in the P-branch of these bands is smaller than in the R-branch, and since it is more difficult to determine the wavenumber beyond which there is significant absorption, the uncertainty in the measurements of the P-branch is greater than in the R-branch.

The 02^02 band of $C^{12}O^{16}O^{18}$ appears in a region which is free of absorption by other bands and its strength could be determined although it is much weaker than some of the other bands. The value given is based on the absorber thickness of the sample containing all the isotopes of C and O. If we assume that the sample contained the natural abundance (0.20%) of O^{18} , the strength should be multiplied by 500 to apply to a sample composed of $C^{12}O^{16}O^{18}$ molecules only. As was the case for the two bands mentioned in the previous paragraph, the uncertainty in the measurement of the P-branch was greater than that in the R-branch. The uncertainty is also relatively high because of the small absorptance by even the largest samples.

By summing the strengths given by Equation (3-4) for all the lines in the P- and R-branches, we see that approximately 48% of the strength is in the P-branch and 52% in the R-branch. We see that this agrees, within experimental error, with the results listed in Table 3-4. Results of measurements given in previous reports^{4,5} by us tend to confirm the validity of this ratio of strength between the two branches $\Sigma \leftarrow \Sigma$ bands.

Portions of the 06^01 band of $C^{12}O_2^{16}$ are overlapped by lines of its associated difference band $07^11 \leftarrow 01^10$ as well as 14^01 and $15^11 \leftarrow 01^10$ bands of $C^{13}O_2^{16}$; therefore, it was not possible to determine the strength by merely integrating $-\ln(T_V)$ over the region covered by the band. In order to account for the $07^11 \leftarrow 01^10$ band, we assumed that its strength was related to that of its associated summation band by Equation (3-5). We further assumed that the strength of each of the lines within this band was given by Equation (3-4) and calculated the contribution of those within the region of integration. The contribution of the two bands of $C^{13}O_2^{16}$ was small and was calculated by assuming that their strengths were related to the strengths of the same bands of $C^{12}O_2^{16}$ band by the ratio of the relative abundances of C^{13} and C^{12} (1.1:100).

The R-branch of the 14^01 band is essentially isolated from other bands; thus its strength could be determined with relatively good accuracy. In order to calculate the strength of the P-branch, the same technique was used to account for the contribution of the $15^11 \leftarrow 01^10$ band as was used

for the 06^0_1 band. The same technique was also used to account for the small amount of absorption by the weaker bands which overlap the 22^0_1 band.

Only a small correction was required to account for the absorption by weak bands overlapping the P-branch of the 30^0_1 band. However, the R-branch of this band is overlapped by the 03^1_2 and the $31^1_1 \leftarrow 01^1_0$ bands. The contribution of the $31^1_1 \leftarrow 01^1_0$ band could be calculated by the use of Equation (3-5); but without spectra in which the resolution was sufficiently good to resolve the lines of the 03^1_2 band, its contribution would be difficult to determine. Therefore, the strength of the R-branch of the 30^0_1 band which is given in Table 3-4 was not determined directly from the spectra. It was obtained by assuming that the ratio of the strength of the R-branch to the P-branch (52/48) mentioned above is valid.

By using more sophisticated techniques and by making use of spectra having considerably better resolution, it would be possible to determine the strengths of more of the bands in this region. However, we have determined the strengths of the more important ones which produce a very large percentage of the absorption in this region.

SECTION 4

TABLE OF TRANSMITTANCES

Table 4-1 consists of values of transmittance, in percent, recorded at intervals of 0.2 cm^{-1} in the region from 5814 to 6604 cm^{-1} . The interval is sufficiently small that an original spectrum could be approximated very closely by plotting the tabulated values and joining the points with straight lines. The first column gives the wavenumber in cm^{-1} , and the second gives the corresponding wavelength in microns. The tables were made by photographing a portion of the computer output which was obtained from the spectra by the technique described in Appendix C of reference 4.

The CO_2 partial pressure p , the equivalent pressure P_e and the absorber thickness u are shown at the top of the column corresponding to each sample. The samples are designated by the same numbers as Table 3-2 and in the spectra in Section 3.

Values are not tabulated over regions of small, but observable, absorptance ($T \approx 1$) for some of the samples. The transmittance is probably greater than 0.98 or 0.99 for even the largest sample (No. 1) at all wavenumbers between 5400 and 6600 cm^{-1} not showing absorption in either Figure 3-1 or 3-2.

THIS PAGE INTENTIONALLY LEFT BLANK

Table with multiple columns containing numerical data, likely a financial or statistical report. The data is organized into rows and columns, with values ranging from 0 to 100.0. The table is rotated 90 degrees counter-clockwise in the image.

Table 4-1 (cont'd)

Source	λ (micron)	Wavelength																				
		1	2	3	4	5	6	7	8	9	10	11	12	13	14	15	16	17	18	19	20	21
τ (4-2)	2.536 $\times 10^0$	2.536 $\times 10^0$	2.530 $\times 10^0$	2.520 $\times 10^0$	2.506 $\times 10^0$	1.660 $\times 10^0$	1.660	1.660	1.660	1.660	1.660	1.660	1.660	2.101 $\times 10^{-1}$	2.200 $\times 10^{-1}$	2.700 $\times 10^{-2}$	7.700 $\times 10^{-2}$	2.700 $\times 10^{-2}$	7.700 $\times 10^{-2}$	6.651 $\times 10^{-1}$	6.651 $\times 10^{-1}$	6.651 $\times 10^{-1}$
$P_{\beta}(4-2)$	3.290 $\times 10^0$	3.290 $\times 10^0$	3.290 $\times 10^0$	3.262 $\times 10^0$	2.657 $\times 10^0$	1.131 $\times 10^0$	1.131	1.131	1.131	1.131	1.136	1.136	1.136	9.989 $\times 10^{-1}$	3.000 $\times 10^{-1}$	1.000	1.000	1.000	1.000	1.311 $\times 10^1$	8.651 $\times 10^1$	8.651 $\times 10^1$
η (4-1+2)	1.100 $\times 10^0$	1.100 $\times 10^0$	1.100 $\times 10^0$	1.100 $\times 10^0$	1.100 $\times 10^0$	1.100 $\times 10^0$	1.100 $\times 10^0$	1.100 $\times 10^0$	1.100 $\times 10^0$	1.100 $\times 10^0$	1.100 $\times 10^0$	1.100 $\times 10^0$	1.100 $\times 10^0$	9.999 $\times 10^{-1}$	9.999	9.999	9.999	9.999	9.999	9.999	9.999	9.999
STP	1.100 $\times 10^0$	1.100 $\times 10^0$	1.100 $\times 10^0$	1.100 $\times 10^0$	1.100 $\times 10^0$	1.100 $\times 10^0$	1.100 $\times 10^0$	1.100 $\times 10^0$	1.100 $\times 10^0$	1.100 $\times 10^0$	1.100 $\times 10^0$	1.100 $\times 10^0$	1.100 $\times 10^0$	9.999 $\times 10^{-1}$	9.999	9.999	9.999	9.999	9.999	9.999	9.999	9.999

Table 4-1 (cont'd)

Series	λ (microns)	1	2	3	4	5	6	7	8	9	10	11	12	13	14	15	16	17	18	19	20	21	22	23	24	25	26	27				
		$\times 100$	$\times 100$	$\times 100$	$\times 100$	$\times 100$	$\times 100$	$\times 100$	$\times 100$	$\times 100$	$\times 100$	$\times 100$	$\times 100$	$\times 100$	$\times 100$	$\times 100$	$\times 100$	$\times 100$	$\times 100$	$\times 100$	$\times 100$	$\times 100$	$\times 100$	$\times 100$	$\times 100$	$\times 100$	$\times 100$	$\times 100$				
1-6050	1-41951	2-4	2-3	1-3	1-2	1-1	1-1	1-0	1-0	1-0	1-0	1-0	1-0	2-30	2-10	1-16	7-70	7-70	7-70	3-87	6-65	6-65	2-34	2-34	2-34	2-34	2-34	2-34	2-34	2-34	2-34	
	1-41951	$\times 10^6$	$\times 10^6$	$\times 10^6$	$\times 10^6$	$\times 10^6$	$\times 10^6$	$\times 10^6$	$\times 10^6$	$\times 10^6$	$\times 10^6$	$\times 10^6$	$\times 10^6$	$\times 10^6$	$\times 10^6$	$\times 10^6$	$\times 10^6$	$\times 10^6$	$\times 10^6$	$\times 10^6$	$\times 10^6$	$\times 10^6$	$\times 10^6$	$\times 10^6$	$\times 10^6$	$\times 10^6$	$\times 10^6$	$\times 10^6$	$\times 10^6$	$\times 10^6$	$\times 10^6$	
1-6050	1-41951	2-4	2-3	1-3	1-2	1-1	1-1	1-0	1-0	1-0	1-0	1-0	1-0	2-30	2-10	1-16	7-70	7-70	7-70	3-87	6-65	6-65	2-34	2-34	2-34	2-34	2-34	2-34	2-34	2-34	2-34	2-34

Table 4-1 (cont'd)

Sams. No.	27 26 25 24 23 22 21 20 19 18 17 16 15 14 13 12 11 10 9 8 7 6 5 4 3 2 1																														
	T x 100	T x 100	T x 100	T x 100	T x 100	T x 100	T x 100	T x 100	T x 100	T x 100	T x 100	T x 100	T x 100	T x 100	T x 100	T x 100	T x 100	T x 100	T x 100	T x 100	T x 100	T x 100	T x 100	T x 100	T x 100	T x 100					
1-50	2.53	2.53	2.50	2.00	1.00	1.00	1.00	1.00	1.00	2.30	2.30	1.16	7.70	7.70	2.87	2.87	2.87	6.65	6.65	2.36	2.36	2.36	2.36	2.36	2.36	2.36	2.36	2.36	2.36		
...		
1-500	1.40051	1.40051	1.40051	1.40051	1.40051	1.40051	1.40051	1.40051	1.40051	36.2	36.2	50.6	70.7	70.7	61.7	61.7	61.7	78.5	78.5	47.3	47.3	47.3	47.3	47.3	47.3	47.3	47.3	47.3	47.3	47.3	
...

Table with multiple columns containing numerical data, organized in rows and columns. The data appears to be a list of values, possibly representing a sequence or a dataset. The values are arranged in a grid-like format, with some rows having more columns than others. The numbers are mostly integers, with some decimal points. The table is very dense and covers most of the page area.

Table 4-1 (cont'd)

Temp. No.	λ	λ	λ	λ	λ	λ	λ	λ	λ	λ	λ	λ	λ	λ	λ	λ	λ	λ	λ	λ
	μ (atm)	μ (atm)	μ (atm)	μ (atm)	μ (atm)	μ (atm)	μ (atm)	μ (atm)	μ (atm)	μ (atm)	μ (atm)	μ (atm)	μ (atm)	μ (atm)	μ (atm)	μ (atm)	μ (atm)	μ (atm)	μ (atm)	μ (atm)
	μ (atm)	μ (atm)	μ (atm)	μ (atm)	μ (atm)	μ (atm)	μ (atm)	μ (atm)	μ (atm)	μ (atm)	μ (atm)	μ (atm)	μ (atm)	μ (atm)	μ (atm)	μ (atm)	μ (atm)	μ (atm)	μ (atm)	μ (atm)
	μ (atm)	μ (atm)	μ (atm)	μ (atm)	μ (atm)	μ (atm)	μ (atm)	μ (atm)	μ (atm)	μ (atm)	μ (atm)	μ (atm)	μ (atm)	μ (atm)	μ (atm)	μ (atm)	μ (atm)	μ (atm)	μ (atm)	μ (atm)
	μ (atm)	μ (atm)	μ (atm)	μ (atm)	μ (atm)	μ (atm)	μ (atm)	μ (atm)	μ (atm)	μ (atm)	μ (atm)	μ (atm)	μ (atm)	μ (atm)	μ (atm)	μ (atm)	μ (atm)	μ (atm)	μ (atm)	μ (atm)
	μ (atm)	μ (atm)	μ (atm)	μ (atm)	μ (atm)	μ (atm)	μ (atm)	μ (atm)	μ (atm)	μ (atm)	μ (atm)	μ (atm)	μ (atm)	μ (atm)	μ (atm)	μ (atm)	μ (atm)	μ (atm)	μ (atm)	μ (atm)

Table with 15 columns and 1000 rows of numerical data. The first column contains a sequence of numbers from 0 to 999. The remaining columns contain various numerical values, some of which are formatted with commas as thousands separators.

Table 4-1 (cont'd)

Wave	1	2	3	4	5	6	7	8	9	10	11	12	13	14	15	16	17	18	19	20	21
λ (microns)	2.50	2.53	2.56	2.59	2.62	2.65	2.68	2.71	2.74	2.77	2.80	2.83	2.86	2.89	2.92	2.95	2.98	3.01	3.04	3.07	3.10
ν (cm ⁻¹)	4000	3950	3900	3850	3800	3750	3700	3650	3600	3550	3500	3450	3400	3350	3300	3250	3200	3150	3100	3050	3000
σ (cm ⁻¹)	1000	1000	1000	1000	1000	1000	1000	1000	1000	1000	1000	1000	1000	1000	1000	1000	1000	1000	1000	1000	1000
τ (cm ⁻¹)	1000	1000	1000	1000	1000	1000	1000	1000	1000	1000	1000	1000	1000	1000	1000	1000	1000	1000	1000	1000	1000
ρ (cm ⁻¹)	1000	1000	1000	1000	1000	1000	1000	1000	1000	1000	1000	1000	1000	1000	1000	1000	1000	1000	1000	1000	1000
μ (cm ⁻¹)	1000	1000	1000	1000	1000	1000	1000	1000	1000	1000	1000	1000	1000	1000	1000	1000	1000	1000	1000	1000	1000
ϵ (cm ⁻¹)	1000	1000	1000	1000	1000	1000	1000	1000	1000	1000	1000	1000	1000	1000	1000	1000	1000	1000	1000	1000	1000
δ (cm ⁻¹)	1000	1000	1000	1000	1000	1000	1000	1000	1000	1000	1000	1000	1000	1000	1000	1000	1000	1000	1000	1000	1000
γ (cm ⁻¹)	1000	1000	1000	1000	1000	1000	1000	1000	1000	1000	1000	1000	1000	1000	1000	1000	1000	1000	1000	1000	1000
β (cm ⁻¹)	1000	1000	1000	1000	1000	1000	1000	1000	1000	1000	1000	1000	1000	1000	1000	1000	1000	1000	1000	1000	1000
α (cm ⁻¹)	1000	1000	1000	1000	1000	1000	1000	1000	1000	1000	1000	1000	1000	1000	1000	1000	1000	1000	1000	1000	1000

Table with multiple columns containing numerical data. The data is organized in a grid-like format with varying column widths and values ranging from 0.0 to 100.0.

Table 4-1 (cont'd)

Wm. No.	1	2	3	4	5	6	7	8	9	10	11	12	13	14	15	16	17	18	19	20	21		
$P(\text{atm})$	2.50×10^0	2.55×10^0	2.60×10^0	2.65×10^0	2.70×10^0	2.75×10^0	2.80×10^0	2.85×10^0	2.90×10^0	2.95×10^0	3.00×10^0	3.05×10^0	3.10×10^0	3.15×10^0	3.20×10^0	3.25×10^0	3.30×10^0	3.35×10^0	3.40×10^0	3.45×10^0	3.50×10^0		
$P_0(\text{atm})$	3.29×10^0	3.32×10^0	3.35×10^0	3.39×10^0	3.42×10^0	3.45×10^0	3.48×10^0	3.51×10^0	3.54×10^0	3.57×10^0	3.60×10^0	3.63×10^0	3.66×10^0	3.69×10^0	3.72×10^0	3.75×10^0	3.78×10^0	3.81×10^0	3.84×10^0	3.87×10^0	3.90×10^0		
$u(\text{cm cm})$	2.17×10^5	1.10×10^5	5.57×10^4	2.80×10^4	8.71×10^3	8.62×10^3	2.19×10^4	3.18×10^4	3.15×10^4	1.59×10^4	7.93×10^3	3.99×10^3	9.84×10^2	9.84×10^2	9.94×10^2	3.32×10^3	3.32×10^3	3.32×10^3	3.32×10^3	3.32×10^3	1.01×10^3	8.65×10^2	
λ (microns)	1.52691	1.52692	1.52693	1.52694	1.52695	1.52696	1.52697	1.52698	1.52699	1.52700	1.52701	1.52702	1.52703	1.52704	1.52705	1.52706	1.52707	1.52708	1.52709	1.52710	1.52711	1.52712	
ν (cm ⁻¹)	6539.6	6539.5	6539.4	6539.3	6539.2	6539.1	6539.0	6538.9	6538.8	6538.7	6538.6	6538.5	6538.4	6538.3	6538.2	6538.1	6538.0	6537.9	6537.8	6537.7	6537.6	6537.5	6537.4
ν (cm ⁻¹)	6539.6	6539.5	6539.4	6539.3	6539.2	6539.1	6539.0	6538.9	6538.8	6538.7	6538.6	6538.5	6538.4	6538.3	6538.2	6538.1	6538.0	6537.9	6537.8	6537.7	6537.6	6537.5	6537.4
ν (cm ⁻¹)	6539.6	6539.5	6539.4	6539.3	6539.2	6539.1	6539.0	6538.9	6538.8	6538.7	6538.6	6538.5	6538.4	6538.3	6538.2	6538.1	6538.0	6537.9	6537.8	6537.7	6537.6	6537.5	6537.4

Table 4-1 (cont'd)

	1	2	3	4	5	6	7	8	9	10	11	12	13	14	15	16	17	18	19	20	21
λ (microns)	$T \times 100$	$T \times 100$	$T \times 100$	$T \times 100$	$T \times 100$	$T \times 100$	$T \times 100$	$T \times 100$	$T \times 100$	$T \times 100$	$T \times 100$	$T \times 100$	$T \times 100$	$T \times 100$	$T \times 100$	$T \times 100$	$T \times 100$	$T \times 100$	$T \times 100$	$T \times 100$	$T \times 100$
A-578.1	86.1	86.1	86.1	86.1	86.1	86.1	86.1	86.1	86.1	86.1	86.1	86.1	86.1	86.1	86.1	86.1	86.1	86.1	86.1	86.1	86.1
A-578.1	86.1	86.1	86.1	86.1	86.1	86.1	86.1	86.1	86.1	86.1	86.1	86.1	86.1	86.1	86.1	86.1	86.1	86.1	86.1	86.1	86.1
A-578.1	86.1	86.1	86.1	86.1	86.1	86.1	86.1	86.1	86.1	86.1	86.1	86.1	86.1	86.1	86.1	86.1	86.1	86.1	86.1	86.1	86.1
A-578.1	86.1	86.1	86.1	86.1	86.1	86.1	86.1	86.1	86.1	86.1	86.1	86.1	86.1	86.1	86.1	86.1	86.1	86.1	86.1	86.1	86.1
A-578.1	86.1	86.1	86.1	86.1	86.1	86.1	86.1	86.1	86.1	86.1	86.1	86.1	86.1	86.1	86.1	86.1	86.1	86.1	86.1	86.1	86.1

Table with 12 columns of numerical data, organized in rows. The values are generally small integers, with some larger numbers appearing in the later rows.

SECTION 5

TABLE OF INTEGRATED ABSORPTANCE

Values of the integrated absorptance over the region from 5814 to 6582 cm^{-1} are presented in Table 5-1 for the samples listed in Table 3-2. The integrals were calculated from the transmittance tables in Section 4 by assuming a spectrum could be constructed by plotting the transmittance values and joining them with straight lines. The important sample parameters are listed at the top of each column corresponding to a given sample.

The lower limit of integration ν' , which is shown at the top of each column, was chosen at a point where there was very little, if any, absorption. ν' is different for some samples than for others, since the integration was not performed over some of the regions of small absorption. The absorption by small samples is negligible in some regions where it is important for large samples.

In regions where the structure in the spectra is regular, the integrated absorptance was calculated at wavenumbers midway between the line centers. Thus, in the case of no overlapping, the difference between two successive tabulated values is the equivalent width of the absorption line in the interval. In some other regions where the structure was not particularly regular, the integrated absorptance was calculated at wavenumbers corresponding to absorptance minima. In still other regions where there was but little structure or where the absorptance minima would shift as the pressure or absorber thickness was changed, the values were calculated at integral wavenumbers, or possibly at integral half-wavenumbers, depending on the amount of information one might expect to obtain from closer readings.

SECTION 6

REFERENCES

1. J. N. Howard, D. E. Burch, and Dudley Williams, J. Opt. Soc. Am. 46, 237, (1956).
2. C. P. Courtoy, Annales de la Societe Scientifique de Bruxelles, Serie 1, pp 5-230 (27 March 1959). Also, C. P. Courtoy, Canad J. Phys. 35, 608 (1957).
3. G. P. Kuiper, Communications of Lunar and Planetary Laboratory, Vol. 1, No. 14-16, Univ. of Arizona Press (1962).
4. D. E. Burch, D. A. Gryvna and R. R. Patty, Absorption of CO₂ Between 4500 and 5400 cm⁻¹, Aeronutronic Report U-2955, Contract NOnr 3560(00), (15 December 1964).
5. D. E. Burch, D. A. Gryvna and R. R. Patty, Absorption by CO₂ Between 6600 and 7125 cm⁻¹ (1.4 Micron Region), Aeronutronic Report U-3127, Contract NOnr 3560(00), (1965).
6. D. E. Burch, D. A. Gryvna and Dudley Williams, Appl. Opt. 1, 759, (1962).
7. D. E. Burch, D. A. Gryvna, R. R. Patty and Charlotte Bartky, The Shapes of Collision-Broadened CO₂ Absorption Lines, Aeronutronic Report U-3203, Contract NOnr 3560(00), (1965).
8. V. R. Stull, P. J. Wyatt and G. N. Plass, The Infrared Absorption of Carbon Dioxide, Aeronutronic Report U-1505, Contract AF 19(604)-7479, (30 December 1961).
9. A Table of Solar Spectrum Wavelengths, Orren C. Mohler, The University of Michigan Press, Ann Arbor, 1955.
10. L. D. Gray and J. E. Selvide, J. Quant. Spectros. Radiat. Transfer 5, 291, (1965).
11. G. Herzberg, Infrared and Raman Spectra of Polyatomic Molecules, D. Van Nostrand Co. (See 266 ff for a discussion of the intensities of difference bands), (Ninth printing 1960).